Tetrahedron: *Asymmetry* 20 (2009) 2130–2136

Contents lists available at ScienceDirect

Tetrahedron: *Asymmetry*

journal homepage: www.elsevier.com/locate/tetasy

From racemic compounds through metastable to stable racemic conglomerates: crystallization features of chiral halogen and cyano monosubstituted phenyl glycerol ethers

Alexander A. Bredikhin *, Zemfira A. Bredikhina, Flyura S. Akhatova, Dmitry V. Zakharychev, Elena V. Polyakova

A.E. Arbuzov Institute of Organic and Physical Chemistry, Russian Academy of Sciences, Arbuzov St., 8, Kazan 420088, Russian Federation

ARTICLE INFO

Article history:
Received 13 July 2009
Accepted 4 September 2009
Available online 30 September 2009

ABSTRACT

All *ortho*-substituted Cl, Br, I, and CN phenyl glycerol ethers crystallize as racemic conglomerates, whereas *meta*- and *para*-derivatives constitute racemic compounds in the solid state. Only *meta*-halogen-substituted phenyl glycerol ethers, alongside the thermodynamically preferential heterochiral racemic compound phase, reveal the simultaneous existence of a conglomerate phase; the last state is metastable and turns into a stable racemic compound just in the crystalline phase.

1. Introduction

Starting with Pasteur's original demonstration of the tartrate (enantiopure) crystal formation during racemic acid salt crystallization,[1] spontaneous resolution has provoked much interest from both theorists and practitioners of organic chemistry. With regard to this phenomenon, all reviewers are in agreement that the present level of theory has given no way to solve the problem of homochiral crystallization against heterochiral crystallization, while the understanding of the factors controlling the two enantiomers' behavior upon solution or melt crystallization is rather limited.[2–4]

In the absence of a rigorous theory, we believe that investigations of the crystal structure changes with chemical structure variations in a series of closely related compounds would be fruitful. The members of such a series must be selected in such a way that every compound would have minimal but regular distinctions from each other. In addition, a quantitative measure, which allows ranking the observed properties for all the compounds studied, would be desirable. In our previous papers, this approach was successfully applied to a series of *o*-halogen,[5] *o*-alkyl,[6] and *o*-alkoxy-substituted[7] phenyl glycerol ethers of the general formula **1**.

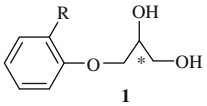

1

Some new ordinary (**1**, R = Cl, Br, I, CH_3, CH_3CH_2, CH_3O, $(CH_3)_2$CHO) or anomalous (**1**, R = $(CH_3)_3C$) conglomerate-forming compounds (i.e., compounds prone to spontaneous resolution) have been revealed during the investigations.

It is easily anticipated that for compounds with at least three strong hydrogen bond acceptors (oxygen atoms) and two hydrogen bond donors (hydroxyl groups), the intermolecular hydrogen bond network would be the main crystal-forming factor. This is indeed the case for X-ray studied conglomerates guaifenesin (**1**, R = CH_3O) and mephenesin (**1**, R = CH_3).[8] Nevertheless, from other experience it follows that some stable conglomerate-forming compounds keep the conglomerate nature even after severe transformations of the hydroxyl-bearing fragments. Thus having no free OH groups, guaifenesin precursor 1,2-epoxy-3-(2-methoxyphenoxy)-propane **2**,[9] and having a rather different set of hydrogen bond-forming fragments related to guaifenesin miorelaxant methocarbamol **3**[8,10] both demonstrate the property of spontaneous resolution.

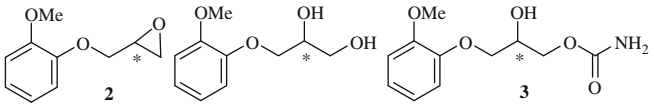

2 guaifenesin **3** methocarbamol

The same is true for conglomerate-forming 3-(2-cyanophenoxy)-propane-1,2-diol (**1**, R = CN): not only this compound by itself, but its hydroxyl-free derivatives, epoxide **4** and sulfate **5**, form stable racemic conglomerates.[11]

* Corresponding author. Tel.: +7 843 2727392; fax: +7 843 2731872.
E-mail address: baa@iopc.knc.ru (A.A. Bredikhin).

0957-4166/$ - see front matter © 2009 Elsevier Ltd. All rights reserved.
doi:10.1016/j.tetasy.2009.09.008

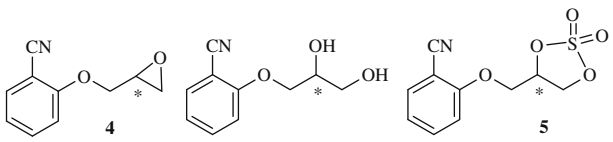

Herein we turn our attention to the close examination of the crystalline state nature for another organized series of aryl glycerol ethers. Instead of changing the nature of substituent at the *ortho*-position of the phenoxy fragment or modifying the vicinal diol fragment, we intend to 'move' the substituent along the phenyl ring, that is, to investigate quantitatively the crystallization features of *ortho*-, *meta*-, and *para*-isomers of the monosubstituted phenyl glycerol ethers. In the beginning, we will use halogens (Cl, Br, and I) and pseudohalogen CN groups as rigid substituents with no conformational issues. As a quantitative measure enables us to compare different compounds we will use the correlation of IR spectra (to a certain extent), and some thermodynamic parameters, such as the Gibbs free energy changes, ΔG^0, accompanied by the reaction of racemic compound formation from the enantiopure components, and the values of entropy of enantiomers mixing in the liquid state, ΔS_l^m.

2. Results and discussion

2.1. Chemistry

All the compounds studied were obtained, via the use of a single process outlined in Scheme 1, from the corresponding phenol and racemic or scalemic 3-chloropropane-1,2-diols.

The main obstacle is the difficulty of the target product separation from the excessive phenol, hence a slight excess of 3-chloropropane-1,2-diol was usually used. In some cases this in turn leads to a small amount of achiral bis-adduct RC_6H_4–O–CH_2–CH(OH)–CH_2–OC_6H_4R formation, but these side products were usually easily separable.

We would like to note that most of the substances investigated here belong to the not so common class of chiral compounds which change the sign of the specific rotation with the solvent change, for example, (*S*)-3-(2-chlorophenoxy)-propane-1,2-diol, (*S*)-**1a**, $[\alpha]_D^{20} = -14.0$ (*c* 1.0, hexane/EtOH 4:1); $[\alpha]_D^{20} = +4.0$ (*c* 1.0, EtOH); $[\alpha]_D^{20} = +8.9$ (*c* 0.7, $CHCl_3$). Dealing with such compounds, one must be careful in using combined descriptors such as (*S*)-(+).

2.2. IR spectra comparison

For the initial evaluation of the crystallization type of our compounds, we compared the IR spectra of the pairs of racemic and highly enantiomerically enriched crystalline samples of **1**, **6**, and **7** in KBr pellets, since the IR spectra of an optically active and the racemic form should be identical for the normal conglomerate formative compounds. However, it is not feasible to prepare two samples (pellets) identical in density, thickness, and homogeneity by routine procedure. For these reasons experimentally measured extinction effective values (linearly concentration dependent) and the non-specific absorption of the matrix material (KBr) could be essentially different from sample to sample.

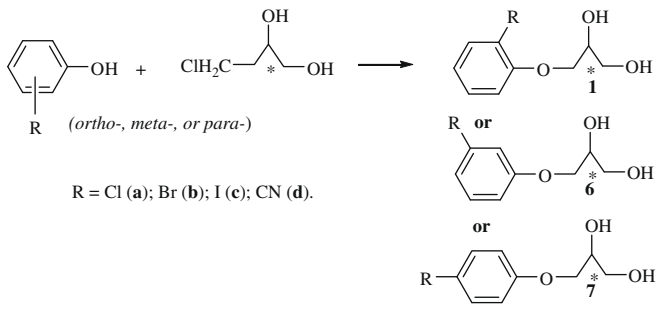

Scheme 1. Synthesis of the chiral monosubstituted phenyl glycerol ethers **1a**–**d**, **6a**–**d**, and **7a**–**d**.

It should be remembered that the real goal of the comparison of racemic and scalemic samples in the content of our investigations is to establish and to quantify *the fact* of similarity or dissimilarity of the spectra, but not to establish *the nature* of dissimilarity. The most direct approach for the purpose is to establish effective correlation criteria between two spectra under comparison. Real modern digital spectra constitute 2D arrays (A_i, ν_i) where ν_i represents vibration frequency (usually specified as wave numbers with a step of one cm^{-1}) and A_i represents extinction corresponding to a given wave number. Thus the quantitative comparison of the spectra of racemic (upper index R) and scalemic (upper index S) samples could be carried out following the standard procedure of Pearson correlation coefficient[12]

$$r(x,y) = \frac{\sum_{i=0}^{n-1}(x_i - \bar{x})\cdot(y_i - \bar{y})}{\sqrt{\sum_{i=0}^{n-1}(x_i - \bar{x})^2 \cdot \sum_{i=0}^{n-1}(y_i - \bar{y})^2}}$$

computation between two vectors $\{A_i^R\}$ and $\{A_i^S\}$. The value $\mathbf{r}(A^R,A^S) = 1$ corresponds to a perfect correlation (identity in our case) of two vectors (spectra), so the quantity $\mathbf{r}' = (1 - \mathbf{r})\cdot 100$ (%) could be treated as a percent of discrepancy between the pair of spectra. The approach proposed is straightforward, has a transparent physical meaning, uses standard mathematics, and needs no preliminary spectra treatment. Following the generally accepted conception of poor correlative arrays if their correlation coefficient $\mathbf{r} \leqslant 0.95$ we will use the value of discrepancy coefficient $\mathbf{r}' \geqslant 5\%$ as a borderline for dividing 'similar' and 'dissimilar' spectra.

The results obtained for the comparison of the pairs of IR spectra of racemic and highly enantiomerically enriched samples of compounds **1a**–**d**, **6a**–**d**, and **7a**–**d**, expressed as the discrepancy coefficients **r**′, are presented in Table 1. From these data the similarity of the paired racemic/scalemic samples spectra for *ortho*-substituted compounds **1** and dissimilarity for the same pairs for *meta*- and *para*-substituted compounds **6** and **7** are recognizable at a glance.

2.3. Thermochemical investigations and phase behavior of the compounds 1, 6, and 7

Differential scanning calorimetry (d.s.c.) has served as a working method for the thermal measurements in this work. The results obtained for the temperature (T^f) and the enthalpy of fusion (ΔH^f) of the pure enantiomers (low index *A*) and the pure racemates (low index *R*) of aryl glycerol ethers **1a**–**d**, **6a**–**d**, and **7a**–**d** are presented in Table 2.

Table 1
The discrepancy coefficients **r**′ (%, see text) between the IR spectra for pairs of solid polycrystalline racemic and highly enantioenriched samples of compounds **1a**–**d**, **6a**–**d**, and **7a**–**d**

Substituent	Compound type		
	1	**6**	**7**
a (Cl)	1.0	9.6	25.5
b (Br)	1.4	23.8	13.5
c (I)	3.9	14.8	29.2
d (CN)	0.4	36.4	24.0

Table 2
D.s.c. measured melting point (T^f) and enthalpy of fusion (ΔH^f) of racemic (low index *R*) and enantiopure (low index *A*) compounds **1a–d**, **6a–d**, and **7a–d** and calculated thermodynamic characteristics for these substances, calculated and measured eutectic (low index eu) fusion temperature, and eutectic enantiomeric composition (*x*—mole fraction of a predominant enantiomer)

Compd	T^f_A (°C)	T^f_R (°C)	ΔH^f_A (KJ mol^{-1})	ΔH^f_R (KJ mol^{-1})	T^f_{eu}, calcd (°C)	T^f_{eu}, exp. (°C)	x_{eu}	ΔS^m_l (J K^{-1} mol^{-1})	ΔG^0 (J·mol^{-1})
1a	90.3	70.7	35.5	31.9	70.0[a]	70.7	0.50	5.3	−67
1b	100.7	81.1	37.1	35.5	80.2[a]	81.1	0.50	5.4	−89
1c	110.0	89.9	39.6	36.1	89.8[a]	89.9	0.50	5.3	−14
1d	72.6	51.1	28.6	26.6	50.1[a]	51.5	0.50	5.2	−126
6a	75.1	66.5	29.3	31.4	52.8[a] 63.6[b]	(53.2) 62.2	(0.50) 0.71	—	−1232
6b	78.9	69.8	28.7	31.5	55.7[a] 66.9[b]	(54.8) 65.2	(0.50) 0.71	—	−1233
6c	76.8	73.3	27.2	32.2	(52.7)[a] 67.7[b]	(53.8) 66.7	(0.50) 0.78	—	−1721
6d	73.4	77.0	29.5	27.5	67.8[b]	67.6	0.76	—	−1694
7a	82.8	79.5	30.3	37.2	74.3[b]	74.8	0.74	—	−1750
7b	90.7	84.7	29.1	35.4	80.3[b]	80.1	0.75	—	−1583
7c	109.4	105.5	36.2	35.8	100.4[b]	101.0	0.76	—	−1814
7d	71.1	100.0	21.7	32.3	69.3[b]	67.9	0.96	—	−4478

[a] Calculated as the intersection for two Schröder–Van Laar curves branches.
[b] Calculated as the intersection for Schröder–Van Laar and Prigogine–Defay curves branches.

In the idealized case, to construct the liquidus of the binary melting phase diagram in the region of a pure component fusion, it is enough to have thermochemical data for an enantiomerically pure sample and to use the simplified form of the Schröder–Van Laar equation[13]

$$\ln x = \frac{\Delta H^f_A}{R}\left(\frac{1}{T^f_A} - \frac{1}{T^f}\right) \quad (1)$$

where *x* is the mole fraction of one of the enantiomers in the mixture; and *R* is the universal gas constant (R = 8.3170 J K^{-1} mol^{-1}). The liquidus lines of the phase diagrams for compounds **1**, **6**, and **7**, which were calculated by Eq. 1 using experimental data for enantiomerically pure diols, are presented in Figure 1 (blue lines). The same figures show the experimentally obtained liquidus points drawn by blue circles. For samples of diols with an intermediate enantiomeric composition, the experimental d.s.c. curves contain additional peaks with the almost constant temperature T^f_{eu} which corresponds to the melting point of the eutectics. These experimental characteristics are present on the plot as solid black circles. It is significant that for compounds **1a–d** experimental liquidus points, including points for racemates, practically fall on the Schröder–Van Laar curves.

The experimental data for racemates, T^f_R and ΔH^f_R, allow us to construct another type of a theoretical curve describing a liquidus line for a congruent melting of binary molecular compounds. In this case, the liquidus line obeys the Prigogine–Defay equation,[13] which is generally used in the simplified form

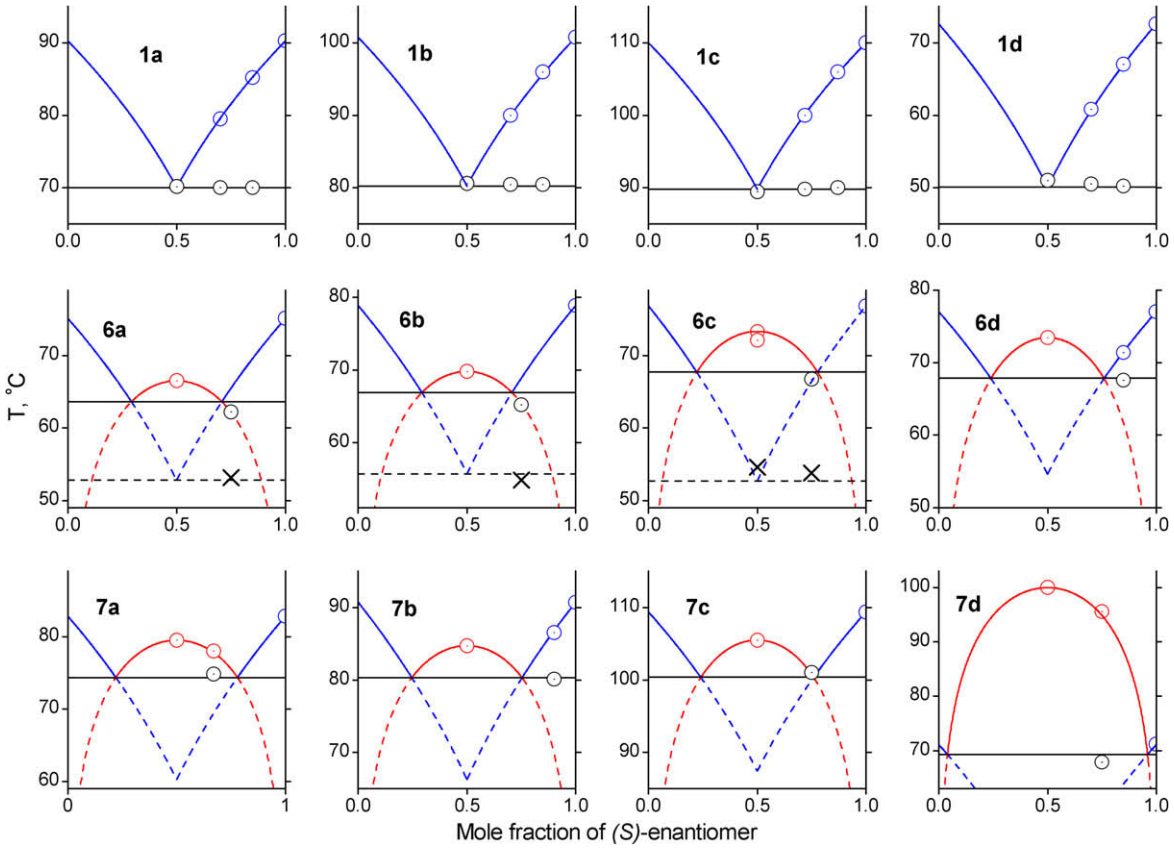

Figure 1. Experimental (circles and crosses) points and calculated (solid lines fragments) binary melting phase diagrams for compounds **1a–d**, **6a–d**, and **7a–d**.

$$\ln 4x(1-x) = \frac{2\Delta H_R^f}{R}\left(\frac{1}{T_R^f} - \frac{1}{T^f}\right) \quad (2)$$

The liquidus lines of the phase diagrams for compounds **1**, **6**, and **7**, which were calculated by Eq. 2 using experimental data for racemic diols, are presented in Figure 1 by red lines. Complete melting phase diagrams could be reproduced by solid liquidus lines fragments with the addition of probable solidus lines (black straight lines which are drawn parallel to the *x*-axis).

Inspecting the forms of so-built phase diagrams one can suppose that the investigated *ortho*-substituted phenyl glycerol ethers **1a–d** crystallize as racemic conglomerates, whereas the *meta*- and *para*-ethers **6** and **7** form solid racemic compounds. There are other points in favor of this distribution of the crystallization types. We took a mean of the free energy of formation of racemic compounds in the solid state, ΔG^0; formulas for this value calculation were proposed by Grant et al.[14]

$$\Delta G^0_{T_R^f} = -\frac{(T_R^f - T_A^f)\Delta H_A^f}{T_A^f} - T_R^f R\ln 2 \quad (\text{if } T_R^f - T_A^f < 0) \quad (3a)$$

$$\Delta G^0_{T_A^f} = -\frac{(T_R^f - T_A^f)\Delta H_R^f}{T_R^f} - T_A^f R\ln 2 \quad (\text{if } T_R^f - T_A^f > 0) \quad (3b)$$

The relatively high negative ΔG^0 value for *para*-cyanosubstituted phenyl glycerol ether **7d** is a diagnostic for a rather stable racemic compound formation in the crystalline state. The moderate negative ΔG^0 values for other *para*-**7a–c** and all *meta*-**6a–d** derivatives indicate the moderately stable racemic compound formations in these cases. The near zero values for ΔG^0 are evidence of no racemic compound generation (in other words, of racemic conglomerate formation) for all the *ortho*-substituted substances **1a–d**.

Another computational parameter for chiral substance crystallization is the entropy of liquid enantiomers mixing, ΔS_l^m, which could be calculated according to the Grant et al. formula.[14]

$$\Delta S_l^m = \frac{\Delta H_R^f}{T_R^f} - \frac{\Delta H_A^f}{T_A^f} - \frac{\Delta H_R^f - \Delta H_A^f}{T_R^f - T_A^f}\ln\frac{T_B^f}{T_A^f} \quad (4)$$

For the system of non-interacting enantiomers, the ΔS_l^m value is equal to $R\ln 2$ (5.75 J K^{-1} mol^{-1}). Substances **1a–d** have ΔS_l^m values similar to this which suggests their conglomerate nature.

It should be noted that the calculated value ΔS_l^m according to Eq. (4) conserves its physical meaning of mixing entropy only for a true conglomerate case (we shall not discuss here some minor problems involving the consideration of the heat capacity changes during the racemate and scalemate fusion). For the racemic compound-forming substances, this term turns into superposition of the proper entropy of enantiomers mixing in the liquid state and the entropy of solid racemic compound formation. For these reasons, the term could be varied through a broad range and even changes sign, so it must not be used (at least under the name of 'mixing entropy') for the characterization of such substances.

Further important information about the compounds under investigation can be obtained by inspection of the characteristics of the binary phase diagram. The case in hand is the composition of the eutectic. The last is the special point on the binary (or ternary) phase diagram where the three phases, liquid (melt or solution) and two solids (either two individual enantiomers or enantiomer and racemic compounds) exist in equilibrium. If the enantiomeric excess of the eutectic point (ee_{eu}) is exactly equal to zero, we deal with a conglomerate-forming compound. For this compound the direct resolution approaches could be realized and enantiomeric composition of *any* scalemic (non-racemic) sample could be enriched to any desirable degree by fraction crystallization. If the eutectic ee lies between 0 and 1 ($0 < ee_{eu} < 100\%$), we deal most likely with a racemic compound-forming substance. For this system, the standard direct resolution is impossible, but if the ee of the starting sample is lower than ee_{eu}, the predominant enantiomer can be enriched in the liquid phase (mother liquor) to the eutectic ee extent, whereas the precipitate will tend to be a racemate. If the solution of the starting material has an ee higher than the ee_{eu}, a pure predominant enantiomer or mixtures of enantiomers with an ee higher than the eutectic ee can be crystallized out. Equilibrium crystallization of the sample with $ee = ee_{eu}$ could not change its enantiomeric composition either in the precipitate or in the filtrate form.

The eutectic compositions for glycerol ethers **1**, **6**, and **7** are presented in Table 2. From this it follows that the sample could be enantioenriched by crystallization provided that its initial enantiomeric excess is similar to or more than 92% (**7d**), 52% (**6c–d**, **7a–c**), and 42% (**6a–b**). For the *ortho*-derivatives **1a–d** a sample could be racemic for the purpose; in other words, these compounds could be potentially resolvable by direct methods.

Of particular interest is the case of *meta*-halogen-substituted phenyl glycerol ethers **6a–c**. The melting of their racemates reveals thermochemical characteristics typical to racemic compounds, so common W-shaped binary phase diagrams (Fig. 1) are quite adequate for these compounds. But freshly prepared samples of near eutectic composition demonstrate anomalous d.s.c. curves. The typical one is reproduced in Figure 2.

As can be seen from Figure 2a, the melting of a freshly prepared, close to eutectic composition, sample of *m*-Br derivative **6b**, alongside the forthcoming strongly pronounced peak of 'normal' eutectic fusion in the temperature region near the cross point of Schröder–Van Laar and Prigogine–Defay curve branches, reveals another endothermic effect in the sufficiently low temperature zone. The temperatures for these effects are included in Table 2 parenthetically and marked in Figure 1 by black crosses. The minor peak reduces over the course of time, and the d.s.c. curve for the sample develops a canonical appearance (Fig. 2b). It should be noted that the temperature region for minor effects is close to the cross point of two Schröder–Van Laar curves for the substances **6a–c**, that is, to the melting point of their hypothetical racemic conglomerates (Table 2).

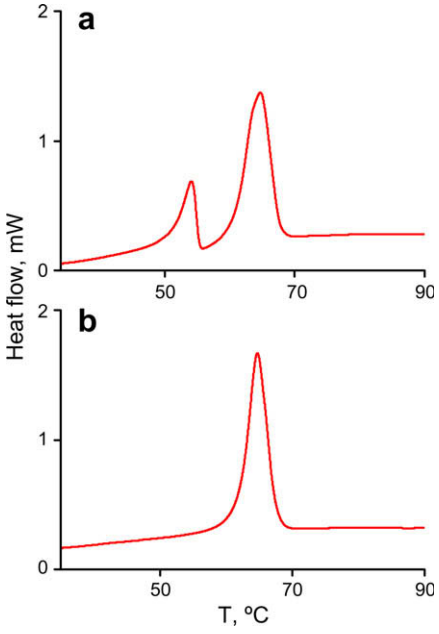

Figure 2. D.s.c. traces for the near eutectic composition samples of 3-(3-bromophenoxy)-propane-1,2-diol **6b**; (a) freshly precipitated sample; (b) the same sample after a week ambient temperature storage.

We believe that the crystallization of the *meta*-substituted compounds **6a**–**c** is kinetically controlled. Thus, despite the fact that racemic compound crystals formation is thermodynamically favorable (which is obvious from negative Gibbs free energy changes accompanying the process), the nucleation of enantiopure crystals takes place more rapidly. The obtainable conglomerate phase is metastable and turns into a stable racemic compound in the solid phase directly after about a week storage of the sample under ambient temperature. Apparently for the close to racemic composition samples the supersaturation against an enantiopure component is hardly achievable owing to low solubility of racemates (high and equal activity of both enantiomeric components) when compared to eutectics. This is a possible reason for not being able to detect the metastable phase for racemates of *m*-Cl and *m*-Br compounds **6a**,**b**. This was achieved only for *m*-I derivative **6c** in a series of hardly reproducible experiments.

3. Conclusion

There is a great deal of common crystallization features within the family of monosubstituted halogen and cyano phenyl glycerol ethers. Whereas all *ortho*-substituted members demonstrate spontaneous resolution crystallizing as stable conglomerates, *meta*- and *para*-derivatives constitute racemic compounds in the solid state. At the same time Cl, Br, and I derivatives are closer to one another than to the set of CN ones. Thus, *para*-cyanophenyl glycerol ether forms a very stable racemic compound, whereas for halogen-containing substances racemic compounds are characterized by moderate and approximately the same stability for *meta*- and *para*-derivatives. Furthermore, only *meta*-halogen-substituted phenyl glycerol ethers, alongside the thermodynamically preferential heterochiral racemic compound phase, reveal the existence of the homochiral conglomerate phase; the last state is metastable and turns into a stable racemic compound in the crystalline phase.

4. Experimental

4.1. General

The NMR spectra were recorded on a Bruker Avance-600 or a Bruker Avance-400 spectrometers in $CDCl_3$ or DMSO-d_6 with TMS or the signals of the solvent as the internal standard. The IR spectra of the polycrystalline samples of *rac*- and *scal*-compounds under investigations in KBr pellets were recorded on a Bruker IFS-66v Fourier-transform spectrometer. Optical rotations were measured on a Perkin–Elmer model 341 polarimeter (concentration *c* is given as g/100 mL). Melting points for general purposes were determined using a Boëtius apparatus and are uncorrected.

The melting curves were measured on a Perkin–Elmer Diamond DSC differential scanning calorimeter in aluminum pans with the rate of heating of 10 °C min^{-1}. The mass of the samples amounted to approximately 2.5 mg. Temperature scale and heat flux were calibrated against the data for indium, phenol, and naphthalene.

HPLC analyses were performed on a Shimadzu LC-20AD system controller.

4.2. Synthesis

Racemic epichlorohydrin, 3-chloropropane-1,2-diol, and substituted phenols are commercially available. (*S*)-3-Chloro-1,2-propanediol was prepared via a Jacobsen kinetic hydrolytic resolution of *rac*-epichlorohydrin.[15] Racemic and (*S*)-diols **1**, **6**, and **7** were synthesized by analogy with a published procedure[6] from corresponding phenol and racemic or (*S*)-3-chloropropane-1,2-diols with 70–84% yield. The properties of enantiopure (99.4% ee) and *rac*-3-(2-cyanophenoxy)-propane-1,2-diols **1d** were described by us earlier;[11] the characteristics of the other investigated diols are given below.

4.2.1. *rac*-3-(2-Chlorophenoxy)-propane-1,2-diol, *rac*-1a

Mp 70–72 °C (CH_2Cl_2/hexane), (lit.[16] mp 71–72 °C). ^{1}H NMR (400 MHz, $CDCl_3$) δ 2.66 (t, J = 5.7 Hz, 1H, CH_2OH), 3.20 (d, J = 4.3 Hz, 1H, CHO*H*), 3.77–3.90 (m, 2H, CH_2OH), 4.05–4.17 (m, 3H, CHO, CH_2O), 6.92 (t, J = 7.2 Hz, 1H, $C^4_{Ar}H$), 6.95 (d, J = 7.9 Hz, 1H, $C^6_{Ar}H$), 7.20 (dt, J = 7.8, 1.2 Hz; 1H, $C^5_{Ar}H$), 7.35 (dd, J = 7.2, 1.4 Hz; 1H, $C^3_{Ar}H$). ^{13}C NMR (100.6 MHz, $CDCl_3$) δ 63.6 (CH_2OH), 70.1 (CH), 70.7 (OCH_2), 113.8 (C^6_{Ar}), 122.0 (C^4_{Ar}), 122.9 (C^{2A}), 127.8 (C^5_{Ar}), 130.2 (C^3_{Ar}), 153.9 (C^1_{Ar}).

4.2.2. (*S*)-3-(2-Chlorophenoxy)-propane-1,2-diol, (*S*)-1a

Mp 90–91 °C (CH_2Cl_2) (lit.[17] mp 87–89 °C); $[\alpha]^{20}_D = -14.0$ (*c* 1.0, hexane/EtOH 4:1); $[\alpha]^{20}_D = +4.0$ (*c* 1.0, EtOH); $[\alpha]^{20}_D = +8.9$ (*c* 0.7, $CHCl_3$); 99.8% ee [chiral HPLC analysis; Daicel Chiralcel OD (0.46 × 25 cm) column; column temperature 27 °C; eluent: hexane/isopropanol/Et_2NH = 95:5:0.1; flow rate: 1.0 ml/min; UV detector 275 nm: t_R = 32.1 min (minor), t_R = 33.7 min (major)]. {Lit.[18] $[\alpha]^{20}_D = -13.4$ (*c* 1.0, hexane/EtOH 4:1), 99% ee}. ^{1}H NMR (600 MHz, $CDCl_3$) δ 2.50 (s, 2H, OH), 3.81 (dd, J = 11.2, 4.5 Hz; 1H, CH_2), 3.88 (dd, J = 11.2, 3.6 Hz; 1H, CH_2), 4.10–4.17 (m, 3H, CHO, CH_2O), 6.93 (t, J = 7.7 Hz, 1H, $C^4_{Ar}H$), 6.95 (d, J = 8.1 Hz, 1H, $C^6_{Ar}H$), 7.22 (dt, J = 7.7, 1.4 Hz; 1H, $C^5_{Ar}H$), 7.37 (dd, J = 7.7, 1.4 Hz; 1H, $C^3_{Ar}H$).

4.2.3. *rac*-3-(3-Chlorophenoxy)-propane-1,2-diol, *rac*-6a

Mp 65–67 °C (hexane); (lit.[19] mp 64–66 °C; lit.[20] mp 68–69 °C). ^{1}H NMR (600 MHz $CDCl_3$) δ 2.31 (br s, 1H, OH), 2.83 (br s, 1H, OH), 3.73 (dd, J = 11.3, 5.5 Hz; 1H, CH_2), 3.83 (dd, J = 11.3, 3.6 Hz; 1H, CH_2), 4.01–4.04 (m, 2H, CH_2O), 4.07–4.12 (m, 1H, CH), 6.79 (m, 1H, $C^6_{Ar}H$), 6.91 (m, 1H, $C^2_{Ar}H$), 6.95 (m, 1H, $C^4_{Ar}H$), 7.19 (t, J = 8.2 Hz, 1H, $C^5_{Ar}H$). ^{13}C NMR (150.9 MHz, $CDCl_3$) δ 63.5 (CH_2OH), 69.4 (OCH_2), 70.3 (CH), 113.0 (C^6_{Ar}), 115.1 (C^2_{Ar}), 121.5 (C^4_{Ar}), 130.3 (C^5_{Ar}), 135.0 (C^3_{Ar}), 159.2 (C^1_{Ar}).

4.2.4. (*S*)-3-(3-Chlorophenoxy)-propane-1,2-diol, (*S*)-6a

Mp 74–76 °C (hexane) (lit.[19] mp 74–76 °C); $[\alpha]^{20}_D = +15.2$ (*c* 0.8, MeOH); $[\alpha]^{20}_D = +13.0$ (*c* 0.5, EtOH); 99.9% ee [chiral HPLC analysis; Daicel Chiralcel OD-RH (0.46 × 15 cm) column; column temperature 29 °C; eluent: isopropanol/water = 1:3; flow rate: 1.0 ml/min; UV detector 275 nm: t_R = 27.4 min (minor), t_R = 29.1 min (major)]; {lit.[18] $[\alpha]^{20}_D = +13.7$ (*c* 1.0, EtOH); lit.[19] $[\alpha]^{20}_D = +11.2$ (*c* 1.0, EtOH)}. ^{1}H NMR (600 MHz $CDCl_3$) δ 1.91 (t, J = 5.87 Hz, 1H, OH), 2.50 (d, J = 4.8 Hz, 1H, OH), 3.72–3.77 (m, 1H, CH_2), 3.81–3.85 (m, 1H, CH_2), 4.00–4.04 (m, 2H, CH_2O), 4.08–4.14 (m, 1H, CH), 6.81 (m, 1H, $C^6_{Ar}H$), 6.92 (m, 1H, $C^2_{Ar}H$), 6.95 (m, 1H, $C^4_{Ar}H$), 7.20 (t, J = 8.1 Hz 1H, $C^5_{Ar}H$). ^{13}C NMR spectrum was identical with that cited above for *rac*-**6a**.

4.2.5. *rac*-3-(4-Chlorophenoxy)-propane-1,2-diol, *rac*-7a

Mp 78–80 °C (hexane) (lit.[19] mp 80 °C); ^{1}H NMR (600 MHz, $CDCl_3$) δ 1.90 (t, J = 5.9 Hz, 1H, OH), 2.50 (d, J = 4.7 Hz, 1H, OH), 3.71–3.77 (m, 1H, CH_2), 3.81–3.87 (m, 1H, CH_2), 3.98–4.05 (m, 2H, CH_2O), 4.06–4.14 (m, 1H, CH), 6.85 (dt, J = 9.0, 5.8 Hz; 2H, $C^{2,6}_{Ar}H$), 7.24 (dt, J = 9.0, 5.8 Hz; 2H, $C^{3,5}_{Ar}H$). ^{13}C NMR (150.9 MHz, $CDCl_3$) δ 63.5 (CH_2OH), 69.5 (OCH_2), 70.3 (CH), 115.8 ($C^{2,6}_{Ar}$), 126.3 (C^4_{Ar}), 129.4 ($C^{3,5}_{Ar}$), 157.0 (C^1_{Ar}).

4.2.6. (*S*)-3-(4-Chlorophenoxy)-propane-1,2-diol, (*S*)-7a

Mp 81–83 °C (hexane) (lit.[19] mp 83 °C); $[\alpha]^{20}_D = +9.8$ (*c* 0.7, MeOH); $[\alpha]^{20}_D = +13.0$ (*c* 0.5, EtOH); 99.2% ee [chiral HPLC analysis; Daicel Chiralpak AD (0.46 × 25 cm) column; column temperature 27 °C; eluent: hexane/isopropanol = 85:15; flow rate: 1.0 ml/min;

UV detector 254 nm: t_R = 11.1 min (minor), t_R = 12.0 min (major)]; {lit.[19] $[\alpha]_D^{20} = +9.9$ (*c* 1.1, MeOH)}. NMR spectra were identical with these cited above for *rac*-**7a**.

4.2.7. *rac*-3-(2-Bromophenoxy)-propane-1,2-diol, *rac*-1b

Mp 80–82 °C (CH_2Cl_2) (lit.[21] mp 82–83 °C). ^{1}H NMR (400 MHz, $CDCl_3$) δ 2.48 (t, *J* = 6.2 Hz, 1H, CH_2OH), 3.05 (d, *J* = 4.8 Hz, 1H, CHO*H*), 3.80–3.91 (m, 2H, C*H*$_2$OH), 4.07–4.18 (m, 3H, CHO, CH_2O), 6.87 (dt, 1H, *J* = 7.5, 1.2 Hz; $C^4_{Ar}H$), 6.91 (dd, *J* = 8.2, 1.4 Hz, 1H, $C^6_{Ar}H$), 7.26 (td, *J* = 7.8, 1.1 Hz; 1H, $C^5_{Ar}H$), 7.53 (dd, *J* = 7.9, 1.7 Hz; 1H, $C^3_{Ar}H$). ^{13}C NMR (100.6 MHz, $CDCl_3$) δ 63.6 (CH_2OH), 70.0 (CH), 70.8 (OCH_2), 112.3 (C^2_{Ar}), 113.6 (C^6_{Ar}), 122.6 (C^4_{Ar}), 128.6 (C^5_{Ar}), 133.3 (C^3_{Ar}), 154.7 (C^1_{Ar}).

4.2.8. (*S*)-3-(2-Bromophenoxy)-propane-1,2-diol, (*S*)-1b

Mp 101–102 °C (CH_2Cl_2); $[\alpha]_D^{20} = -13.8$ (*c* 1.0, hexane/EtOH 4:1); $[\alpha]_D^{20} = +9.0$ (*c* 1.0, $CHCl_3$); 99.5% ee [chiral HPLC analysis; Daicel Chiralpak AD-RH (0.46 × 15 cm) column; column temperature 29 °C; eluent: isopropanol/water = 1:3; flow rate: 0.4 ml/min; UV detector 275 nm: t_R = 22.6 min (minor), t_R = 29.2 min (major)]; {lit.[22] for (*R*)-**1b**: mp 98 °C, $[\alpha]_D^{20} = -9.7$ (*c* 1.08, $CHCl_3$), 100% ee}. ^{1}H NMR (600 MHz, $CDCl_3$) δ 2.20 (br s, 2H, OH), 3.84 (dd, *J* = 11.2, 4.5 Hz; 1H, CH_2), 3.89 (dd, *J* = 11.3, 4.0 Hz, 1H, CH_2), 4.10–4.18 (m, 3H, CHO, CH_2O), 6.87 (t, 1H, *J* = 8.1 Hz, $C^4_{Ar}H$), 6.92 (d, *J* = 8.1 Hz, 1H, $C^6_{Ar}H$), 7.27 (t, *J* = 7.7 Hz, 1H, $C^5_{Ar}H$), 7.54 (d, *J* = 7.7 Hz, 1H, $C^3_{Ar}H$).

4.2.9. *rac*-3-(3-Bromophenoxy)-propane-1,2-diol, *rac*-6b

Mp 68–70 °C (hexane); ^{1}H NMR (600 MHz $CDCl_3$) δ 1.90 (t, *J* = 5.9 Hz, 1H, OH), 2.50 (d, *J* = 4.8 Hz, 1H, OH), 3.71–3.77 (m, 1H, CH_2), 3.81–3.87 (m, 1H, CH_2), 4.01–4.05 (m, 2H, CH_2O), 4.06–4.11 (m, 1H, CH), 6.85 (dt, *J* = 8.1, 1.5 Hz; 1H, $C^6_{Ar}H$), 7.08–7.17 (m, 3H, $C^{2,4,5}_{Ar}H$). ^{13}C NMR (150.9 MHz, $CDCl_3$) δ 63.5 (CH_2OH), 69.4 (OCH_2), 70.2 (CH), 113.5 (C^6_{Ar}), 118.0 (C^2_{Ar}), 122.9 (C^4_{Ar}), 124.5 (C^3_{Ar}), 130.6 (C^5_{Ar}), 159.2 (C^1_{Ar}). Anal. Calcd for $C_9H_{11}BrO_3$: C, 43.74; H, 4.46. Found: C, 43.52; H, 4.24.

4.2.10. (*S*)-3-(3-Bromophenoxy)-propane-1,2-diol, (*S*)-6b

Mp 78–79 °C (hexane/benzene); $[\alpha]_D^{20} = +10.0$ (*c* 1.0, EtOH); 99.9% ee [chiral HPLC analysis; Daicel Chiralpak AD (0.46 × 25 cm) column; column temperature 27 °C; eluent: hexane/isopropanol = 95:5; flow rate: 1.0 ml/min; UV detector 254 nm: t_R = 24.3 min (minor), t_R = 25.9 min (major)]. NMR spectra were identical with that cited above for *rac*-**6b**. Anal. Calcd for $C_9H_{11}BrO_3$: C, 43.74; H, 4.46. Found: C, 44.05; H, 4.62.

4.2.11. *rac*-3-(4-Bromophenoxy)-propane-1,2-diol, *rac*-7b

Mp 84–86 °C (hexane/benzene), (lit.[23] mp 82 °C). ^{1}H NMR (600 MHz $CDCl_3$) δ, 1.90 (t, *J* = 6.0 Hz, 1H, OH), 2.50 (d, *J* = 4.8 Hz, 1H, OH), 3.71–3.77 (m, 1H, CH_2) 3.81–3.85 (m, 1H, CH_2), 4.00–4.03 (m, 2H, CH_2O), 4.07–4.13 (m, 1H, CH), 6.79 (dt, *J* = 8.8, 5.5 Hz; 2H, $C^{2,6}_{Ar}H$), 7.38 (dt, *J* = 8.8, 5.5 Hz; 2H, $C^{3,5}_{Ar}H$). ^{13}C NMR (150 MHz, $CDCl_3$) δ 63.5 (CH_2OH), 69.4 (OCH_2), 70.2 (CH), 113.5 (C^4_{Ar}), 116.3 ($C^{2,6}_{Ar}$), 132.4 ($C^{3,5}_{Ar}$), 157.6 (C^1_{Ar}).

4.2.12. (*S*)-3-(4-Bromophenoxy)-propane-1,2-diol, (*S*)-7b

Mp 88–90 °C (hexane/benzene); $[\alpha]_D^{20} = +9.1$ (*c* 0.6, EtOH); 92.2% ee [chiral HPLC analysis; Daicel Chiralpak AD (0.46 × 25 cm) column; column temperature 27 °C; eluent: hexane/isopropanol = 85/15; flow rate: 1.0 ml/min; UV detector 275 nm: t_R = 11.6 min (minor), t_R = 12.6 min (major)]. NMR spectra were identical with that cited above for *rac*-**7b**. Anal. Calcd for $C_9H_{11}BrO_3$: C, 43.74; H, 4.46. Found: C, 43.38; H, 4.29.

4.2.13. *rac*-3-(2-Iodophenoxy)-propane-1,2-diol, *rac*-1c

Mp 90–92 °C (CH_2Cl_2), (lit.[24] mp 95 °C). ^{1}H NMR (400 MHz, $CDCl_3$) δ 2.26 (br s, 2H, OH), 3.85 (dd, *J* = 11.7, 4.5 Hz; 1H, C*H*$_2$OH), 3.90 (dd, *J* = 11.7, 3.8 Hz; 1H, C*H*$_2$OH), 4.07–4.17 (m, 3H, CHO, CH_2O), 6.75 (dt, *J* = 7.6, 1.0 Hz; 1H, $C^4_{Ar}H$), 6.84 (dd, *J* = 8.1, 1.3 Hz, 1H, $C^6_{Ar}H$), 7.77 (dd, *J* = 7.9, 1.4 Hz, 1H, $C^3_{Ar}H$), 7.31 (dt, *J* = 7.8, 1.1 Hz; 1H, $C^5_{Ar}H$). ^{13}C NMR (100.6 MHz, $CDCl_3$) δ 63.7 (CH_2OH), 70.1 (CH), 70.9 (OCH_2), 86.8 (C^2_{Ar}), 112.6 (C^6_{Ar}), 123.3 (C^4_{Ar}), 129.7 (C^5_{Ar}), 139.4 (C^3_{Ar}), 156.9 (C^1_{Ar}).

4.2.14. (*S*)-3-(2-Iodophenoxy)-propane-1,2-diol, (*S*)-1c

Mp 110–112 °C (CH_2Cl_2); $[\alpha]_D^{20} = -16.3$ (*c* 1.0, hexane/EtOH 4:1); 99.9% ee [chiral HPLC analysis; Daicel Chiralpak AD-RH (0.46 × 15 cm) column; column temperature 29 °C; eluent: isopropanol/water = 1:3; flow rate: 0.4 ml/min; detector: 275 nm: t_R = 33.6 min (minor), t_R = 39.2 min (major)]; {lit.[5] $[\alpha]_D^{20} = -15.9$ (*c* 1, hexane/EtOH 4:1)}. ^{1}H NMR (600 MHz, $CDCl_3$) δ 2.26 (br s, 2H, OH), 3.84 (dd, *J* = 11.2, 4.5 Hz; 1H, CH_2), 3.90 (dd, *J* = 11.2, 4.0 Hz, 1H, CH_2), 4.08–4.11 (m, 1H, CHO), 4.13–4.13 (m, 2H, CH_2O), 6.75 (t, 1H, *J* = 7.7 Hz, $C^4_{Ar}H$), 6.84 (d, *J* = 8.6 Hz, 1H, $C^6_{Ar}H$), 7.30 (t, *J* = 7.7 Hz, 1H, $C^5_{Ar}H$), 7.77 (d, *J* = 7.7 Hz, 1H, $C^3_{Ar}H$).

4.2.15. *rac*-3-(3-Iodophenoxy)-propane-1,2-diol, *rac*-6c

Mp 71–73 °C. ^{1}H NMR (600 MHz $CDCl_3$) δ 1.98 (br s, 1H, OH), 2.18 (d, *J* = 4.1 Hz, 1H, OH), 3.75 (m, *J* = 11.4, 5.5, 5.9 Hz; 1H, CH_2), 3.84–3.86 (m, 1H, CH_2), 4.01–4.06 (m, 2H, CH_2O), 4.10–4.13 (m, 1H, CH), 6.90 (dd, *J* = 1.8, 2.3 Hz; 1H, $C^6_{Ar}H$), 7.01 (t, *J* = 8.1 Hz, 1H, $C^2_{Ar}H$), 7.29 (dd, *J* = 1.4, 2.3 Hz; 1H, $C^4_{Ar}H$), 7.33 (d, *J* = 7.6 Hz, 1H, $C^5_{Ar}H$). ^{13}C NMR (150.9 MHz, $CDCl_3$) δ 63.5 (CH_2OH), 69.4 (OCH_2), 70.3 (CH), 94.6 (C^3_{Ar}), 114.2 (C^6_{Ar}), 123.8 (C^2_{Ar}), 130.5 (C^4_{Ar}), 130.9 (C^5_{Ar}), 159.0 (C^1_{Ar}). Anal. Calcd for $C_9H_{11}IO_3$: C, 36.75; H, 3.74. Found: C, 37.02; H, 3.57.

4.2.16. (*S*)-3-(3-Iodophenoxy)-propane-1,2-diol, (*S*)-6c

Mp 76–77 °C (hexane/benzene); $[\alpha]_D^{20} = +11.5$ (*c* 0.5, EtOH); 97.2% ee [chiral HPLC analysis; Daicel Chiralcel OD-RH (0.46 × 15 cm) column; column temperature 40 °C; eluent: isopropanol/water = 1:3; flow rate: 1.0 ml/min; detector: 275 nm: t_R = 52.8 min (minor), t_R = 56.3 min (major)]. ^{1}H NMR (600 MHz, $CDCl_3$) δ 1.90 (t, *J* = 5.9 Hz, 1H, OH), 2.49 (d, *J* = 4.8 Hz, 1H, OH), 3.75 (m, *J* = 11.4, 5.5, 5.9 Hz; 1H, CH_2), 3.85 (m, 1H, CH_2), 4.01–4.04 (m, 2H, CH_2O), 4.07–4.13 (m, 1H, CH), 6.89 (d, *J* = 8.1 Hz, 1H, $C^6_{Ar}H$), 6.99 (dd, *J* = 7.7, 8.4 Hz; 1H, $C^5_{Ar}H$), 7.27–7.29 (m, 1H, $C^2_{Ar}H$), 7.33 (dt, *J* = 1.1, 1.5 Hz; 1H, $C^4_{Ar}H$). ^{13}C NMR spectrum was identical with that cited above for *rac*-**6c**. Anal. Calcd for $C_9H_{11}IO_3$: C, 36.75; H, 3.74. Found: C, 37.07; H, 4.09.

4.2.17. *rac*-3-(4-Iodophenoxy)-propane-1,2-diol, *rac*-7c

Mp 105–107 °C, (lit.[25] mp 106–107 °C). ^{1}H NMR (600 MHz, $CDCl_3$) δ 1.94 (t, *J* = 5.9 Hz, 1H, OH), 2.53 (d, *J* = 5.1 Hz, 1H, OH), 3.74 (m, *J* = 11.4, 5.2 Hz; 1H, CH_2) 3.82–3.85 (m, 1H, CH_2), 3.98–4.03 (m, 2H, CH_2O), 4.08–4.12 (m, 1H, CH), 6.69 (dt, *J* = 5.1, 8.8 Hz; 2H, $C^{2,6}_{Ar}H$), 7.56 (dt, *J* = 5.1, 9.2 Hz; 2H, $C^{3,5}_{Ar}H$). ^{13}C NMR (150.9 MHz, $CDCl_3$) δ 63.5 (CH_2OH), 69.3 (OCH_2), 70.3 (CH), 83.5 (C^4_{Ar}), 117.0 ($C^{2,6}_{Ar}$), 138.4 ($C^{3,5}_{Ar}$), 158.4 (C^1_{Ar}).

4.2.18. (*S*)-3-(4-Iodophenoxy)-propane-1,2-diol, (*S*)-7c

Mp 107–109 °C (hexane/benzene); $[\alpha]_D^{20} = +9.0$ (*c* 0.8, EtOH); 99.5% ee [chiral HPLC analysis; Daicel Chiralpak AD (0.46 × 25 cm) column; column temperature 27 °C; eluent: hexane/isopropanol = 85/15; flow rate: 1.0 ml/min; UV detector 275 nm: t_R = 10.9 min (minor), t_R = 11.7 min (major)]; NMR spectra were identical with that cited above for *rac*-**7c**. Anal. Calcd for $C_9H_{11}IO_3$: C, 36.75; H, 3.74. Found: C, 36.52; H, 3.79.

4.2.19. *rac*-3-(3-Cyanophenoxy)-propane-1,2-diol, *rac*-6d

Mp 75–77 °C (CH_2Cl_2). ^{1}H NMR (600 MHz, $CDCl_3$) δ 1.97 (t, *J* = 5.5 Hz, 1H, OH), 2.55 (d, *J* = 4.4 Hz, 1H, OH), 3.76 (dd, *J* = 11.0, 5.1 Hz; 1H, OCH_2), 3.86 (dd, *J* = 11.0, 4.4 Hz; 1H, OCH_2), 4.06–4.08 (m, 2H, OCH_2), 4.10–4.16 (m, 1H, OCH), 7.14–7.17 (m, 2H, $C^{2,6}_{Ar}H$),

7.26 (s, 1H, $C^4_{Ar}H$), 7.38 (t, J = 7.7 Hz, 1H, $C^5_{Ar}H$). ^{13}C NMR (150.9 MHz, $CDCl_3$) δ 64.8 (CH_2OH), 70.9 (OCH_2), 71.6 (CH), 114.9 (C^3_{Ar}), 119.1 (C^2_{Ar}), 119.9 (CN), 121.1 (C^6_{Ar}), 126.5 (C^4_{Ar}), 131.9 (C^5_{Ar}), 160.0 (C^1_{Ar}). Anal. Calcd for $C_{10}H_{11}NO_3$: C, 62.17; H, 5.73; N, 7.25. Found: C, 62.19; H, 5.85; N, 7.33.

4.2.20. (*S*)-3-(3-Cyanophenoxy)-propane-1,2-diol, (*S*)-6d

Mp 73–75 °C (EtOAc); $[\alpha]^{20}_D = +19.1$ (c 0.74, EtOH); 99.9% ee [chiral HPLC analysis; Daicel Chiralpak AD (0.46 × 25 cm); column temperature 27 °C; eluent: isopropanol/hexane = 15:85; flow rate: 1.0 ml/min;. t_R = 17.1 min (minor), t_R = 18.3 min (major)]. ^1H NMR (600 MHz, $CDCl_3$) δ 2.06 (broad s, 1H, OH), 2.62 (broad s, 1H, OH), 3.75 (dd, J = 11.0, 5.1 Hz; 1H, OCH_2), 3.84 (dd, J = 11.0, ~3.0 Hz; 1H, OCH_2), 4.04–4.08 (m, 2H, OCH_2), 4.10–4.15 (m, 1H, OCH), 7.14–7.16 (m, 2H, $C^{2,6}_{Ar}H$), 7.25 (s, 1H, $C^4_{Ar}H$), 7.37 (dd, J = 8.1, 7.7 Hz, 1H, $C^5_{Ar}H$). ^{13}C NMR spectrum was identical with that cited above for *rac*-**6d**. Anal. Calcd for $C_{10}H_{11}NO_3$: C, 62.17; H, 5.73; N, 7.25. Found: C, 62.43; H, 5.69; N, 7.14.

4.2.21. *rac*-3-(4-Cyanophenoxy)-propane-1,2-diol, *rac*-7d

Mp 100–101 °C (EtOAc). (lit.[26] mp 95–98 °C). ^{13}C NMR (150.9 MHz, DMSO-d_6) δ 64.4 (CH_2OH), 71.6 (OCH_2), 72.0 (CH), 104.6 (C^4_{Ar}), 117.5 ($C^{6,2}{}_{Ar}$), 121.0 (CN), 136.0 ($C^{3,5}_{Ar}$), 164.2 (C^1_{Ar}).

4.2.22. (*S*)-3-(4-Cyanophenoxy)-propane-1,2-diol, (*R*)-7d

Mp 70–72 °C (EtOAc); $[\alpha]^{20}_D = +14.4$ (c 0.7, EtOH); 92.6% ee [Chiral HPLC analysis; Daicel Chiralpak AD (0.46 × 25 cm) column; column temperature 27 °C; eluent: hexane/isopropanol = 90/10; t_R = 39.9 min (minor), t_R = 42.2 min (major)]; {sf. lit.[27] $[\alpha]^{20}_D = +28.2$ (c 0.44, EtOH)}. ^1H NMR (600 MHz, DMSO-d_6) δ 2.40 (br s, 1H, OH), 3.40–3.43 (m, 3H, CH_2OH), 3.78 (m, 1H, CHO), 3.94 (dd, J = 10.3, 6.2 Hz; 1H, OCH_2), 4.07 (dd, J = 10.3, 3.9 Hz; 1H, OCH_2), 7.1 (d, J = 8.8 Hz, 2H, $C^{2.6}_{Ar}H$), 7.72 (d, J = 8.4 Hz, 2H, $C^{3.5}_{Ar}H$). ^{13}C NMR spectrum was identical with that cited above for *rac*-**7d**. Anal. Calcd for $C_{10}H_{11}NO_3$: C, 62.17; H, 5.73; N, 7.25. Found: C, 62.37; H, 5.59; N, 7.21.1.

Acknowledgments

The authors are indebted to Dr. A.V. Pashagin for chiral chromatography measurements. The authors thank the Russian Fund of Basic Research for financial support (Grant number 09-03-00308).

References

1. Pasteur, L. *Ann. Chim. Phys.* **1848**, *24*, 442–460.
2. Levkin, P. A.; Torbeev, V. Y.; Lenev, D. A.; Kostyanovsky, R. G. *Top. Stereochem.* **2006**, *25*, 81–134.
3. Coquerel, G. *Top. Curr. Chem.* **2007**, *269*, 1–51.
4. Perez-Garcia, L.; Amabilino, D. V. *Chem. Soc. Rev.* **2007**, *36*, 941–967.
5. Zakharychev, D. V.; Lazarev, S. N.; Bredikhina, Z. A.; Bredikhin, A. A. *Russ. Chem. Bull .Int. Ed.* **2006**, *55*, 230–237.
6. Bredikhin, A. A.; Bredikhina, Z. A.; Novikova, V. G.; Pashagin, A. V.; Zakharychev, D. V.; Gubaidullin, A. T. *Chirality* **2008**, *20*, 1092–1103.
7. Bredikhin, A. A.; Bredikhina, Z. A.; Zakharychev, D. V.; Konoshenko, L. V. *Tetrahedron: Asymmetry* **2007**, *18*, 1964–1970.
8. Bredikhin, A. A.; Gubaidullin, A. T.; Bredikhina, Z. A.; Krivolapov, D. B.; Pashagin, A. V.; Litvinov, I. A. *J. Mol. Struct.* **2009**, *20*, 377–382.
9. Bredikhin, A. A.; Strunskaya, E. I.; Zakharychev, D. V.; Krivolapov, D. B.; Litvinov, I. A.; Bredikhina, Z. A. *Tetrahedron: Asymmetry* **2005**, *16*, 3361–3366.
10. Bredikhin, A. A.; Bredikhina, Z. A.; Zakharychev, D. V.; Pashagin, A. V. *Tetrahedron: Asymmetry* **2007**, *18*, 1239–1244.
11. Bredikhina, Z. A.; Akhatova, F. S.; Zakharychev, D. V.; Bredikhin, A. A. *Tetrahedron: Asymmetry* **2008**, *19*, 1429–1434.
12. Lomax, R.G. *An Introduction to Statistical Concepts*; Routledge, 2007, 182–183.
13. Jacques, J.; Collet, A.; Wilen, S. H.. *Enantiomers, Racemates and Resolutions*; Krieger Publishing Company:: Malabar, Florida, 1994. 447 pp.
14. Li, Z. J.; Zell, M. T.; Munson, E. J.; Grant, D. J. W. *J. Pharm. Sci.* **1999**, *88*, 337–346.
15. Schaus, S. E.; Brandes, B. D.; Larrow, J. F.; Tokunaga, M.; Hansen, K. B.; Gould, A. E.; Furrow, M. E.; Jacobsen, E. N. *J. Am. Chem. Soc.* **2002**, *124*, 1307–1315.
16. Ludwig, B. J.; West, W. A.; Currie, W. E. *J. Am. Chem. Soc.* **1952**, *74*, 1935–1939.
17. Seki, T.; Takezaki, T.; Ohuchi, R.; Saitoh, M.; Ishimori, T.; Yasuda, K. *Chem. Pharm. Bull.* **1995**, *43*, 1719–1723.
18. Theil, F.; Weidner, J.; Ballschuh, S.; Kunath, A.; Schick, H. *J. Org. Chem.* **1994**, *59*, 388–393.
19. Bredikhin, A. A.; Bredikhina, Z. A.; Lazarev, S. N.; Savel'ev, D. V. *Mendeleev Commun.* **2003**, *13*, 104–105.
20. Yale, H. L.; Pribyl, E. J.; Braker, W.; Bergeim, F. H.; Lott, W. A. *J. Am. Chem. Soc.* **1950**, *72*, 3710–3716.
21. GB Pat. 628497; *Chem. Abstrs*. **1950**, *44*, 3023d.
22. Kuwabe, S.; Torraca, K.; Buchwald, S. *J. Am. Chem. Soc.* **2001**, *123*, 12202–12206.
23. Koelbel, M.; Beyersdorff, T.; Tschierske, C.; Diele, S.; Kain, J. *Chem. Eur. J.* **2000**, *6*, 3821–3837.
24. Brenans, P. *Bull. Soc. Chim. Fr.* **1913**, *13*, 533–537.
25. Radek, O.; Nemecek, O. *Cesk Farm* **1964**, *13*, 456–459.
26. Wagner, G.; Horn, H. *Pharmazie* **1975**, *30*, 353–357.
27. Wang, Z.-M.; Zhang, X.-L.; Sharpless, K. B. *Tetrahedron Lett.* **1993**, *34*, 2267–2270.